How to avoid artefacts in surface photovoltage measurements: A case study with halide perovskites

Igal Levine[1], Gary Hodes[1], Henry J. Snaith[2] and Pabitra K. Nayak[2]

[1]*Dept. of Materials & Interfaces, Weizmann Inst. of Science, Rehovot, Israel, 76100*

[2]*Clarendon Laboratory, Dept. of Physics, Univ. of Oxford, Oxford, UK, OX1 3PU*

Surface Photovoltage Spectroscopy (SPS) is a well-known experimental technique used to evaluate several semiconductor parameters by measuring the work function of the surface of the semiconductor as a function of the incident light wavelength[1,2,3] . This technique can yield valuable information on the existence of traps within the band gap and their relative positions with respect to the band edges, as well as the efficiency of charge separation within a given junction.[1]

SPS has been used to screen and optimize materials and junctions composed of halide perovskite absorbers[4,5,6] particularly with regard to the presence of intra-bandgap states which are expected to be detrimental to the performance of these materials in devices. However, sometimes one can encounter false positive signals in SPS measurements and care has to be taken to eliminate (or at least recognize) such signals. Herein, we give examples of false positive signals, discuss their origin and also provide ways to mitigate them so that the technique can be used as a powerful tool to screen and characterize semiconductor devices and interfaces in a reliable manner.

We refer to an article by Barnea-Nehoshtan et al.[4] that reports SPS measurements on the methyl ammonium Pb(II) iodide (MAPI) system, where an SPV signal is detected in the sub-bandgap region of the material (around 1100 nm, ~1.1 eV from one of the band-edges). We show the result from a repeat experiment in Fig. 1a using the same setup that was used in reference 4, which includes a 690 nm cutoff (longpass) filter inserted for wavelengths longer than 860 nm. The purpose of this filter is to remove second harmonic radiation (half the wavelength of the nominal monochromator wavelength at any setting). Without this filter, second harmonic radiation might give a signal in the sub-bandgap region. Such filtering is standard practice when a grating monochromator is used.

From Fig. 1a, we see two features: One is the step seen at approx. λ = 780 nm, which corresponds to supra-bandgap excitation, (MAPI has a direct band gap of ~1.6 eV and therefore its optical absorption starts at ~780 nm[7,8]) and we denote this wavelength as $\lambda_{bandgap}$. The second feature, which is the focus of this commentary, is peak-shaped, centered at about λ = 1100 nm. The direction of surface photovoltage

(SPV), where SPV is the difference in the contact potential difference (CPD) in the dark and in the light, is positive for both features. This is the expected direction when a transition occurs from an occupied state, either in the valence band or in the band gap, to the conduction band followed by charge separation, e.g. an electron transfer to the electron transport material (ETM), TiO_2 in this specific case, and accumulation of excess holes at the MAPI surface.

The most obvious initial explanation for the sub-bandgap peak would seem to be that photons with sub-bandgap energy (< 1.6 eV) created free carriers in the material, which upon charge separation causes the sub-bandgap SPV peak between 1020 and 1200 nm. While it is tempting to interpret this sub-bandgap response as due to a band of surface states lying between 1.04 eV and 1.22 eV (corresponding to 1200 nm and 1020 nm) below the conduction band, such a distribution of states would give not a peak SPV but rather a knee, as explained in Fig. 2 and in reference 1, except in certain circumstances described later. The transition from localized states inside the band gap (we choose to present them above the valence band in the schematic diagram, Fig. 2a) to the conduction band (or from band tail states in the valence band to the conduction band) can still occur with higher energy photons, as there is a continuum of states inside the conduction band. As a result, the SPV signal should not drop for the higher energy photons, and therefore should appear as a knee as we show in the schematic diagram of Fig. 2b, and ***not*** as a peak, as seen in the experimental spectrum in Fig. 1a.

The SPV signal can appear as a peak if for some reason the incident light intensity drops sharply at a certain wavelength range. An example of this is shown in Fig. 1b which is an SPV spectrum (taken using a completely different SPS setup than used for Fig. 1a) of a of SnO_2/$FA_{0.85}MA_{0.15}PbI_{0.85}Br_{0.15}$/spiro OmeTAD cell, taken using a supercontinuum white light source where the output drops sharply at ~ 450 nm. In the spectrum taken without using any filter, the broad peak mainly between 900 nm and 1050 nm arises from the second order harmonic of the nominal beam. The drop at the high energy side of this peak (~900 nm) corresponds to twice the wavelength of the ~450 nm sharp drop in the source intensity to nearly zero. When a second order filter that covers this region (665 nm longpass filter) is used, the peak disappears and is therefore recognized as a second order artefact.

When the output radiation from the monochromator used to obtain the data shown in Fig. 1a was measured, we were surprised to find that, besides the second and third order harmonics, fractional harmonics (2λ/3 and 2λ/5) were also present. All the measured harmonics are shown in Fig. 3 for three different set wavelengths and with no filters used. The vertical broken green line represents the bandgap of the MAPI. If we consider the 2λ/3 signals (all the higher harmonics will be filtered out by the 690 nm longpass filter used to collect the spectrum in Fig. 1a), then among the three set wavelengths shown in

Fig. 3, the 1100 nm one will produce a 2λ/3 harmonic of higher energy (centered at 773 nm) than the MAPI bandgap and will therefore give an apparently valid signal that is in fact an artefact of the fractional harmonic produced by this apparently defected grating. The 1300 nm set wavelength will give a 2λ/3 wavelength ~872 nm that will not be absorbed by the MAPI. The 1200 nm set wavelength also should not give a 2λ/3 wavelength that can be absorbed by the MAPI according to Fig. 3; however, since the MAPI bandgap varies somewhat in the literature, the onset of absorption is not the same (but slightly redshifted) as the bandgap due to some tailing and the resolution of the monochromator results in a spread of wavelengths. In that case some small signal might still be observed. The sub-bandgap peak in Fig. 1a extends from 1025 nm to 1200 nm. These limits are defined by the 2λ/3 wavelengths of these two limits, i.e. ~683 nm and ~800 nm respectively. The former cutoff is due to the 690 nm longpass filter used while the latter is the limit of absorption by the MAPI. This explains why a peak is observed.

According to this reasoning, a longpass filter that cuts out the 2λ/3 component but not the actual sub-bandgap peak region should also cut out the peak. To verify that indeed this is the case, we recorded the SPV spectrum by putting a 1025 nm longpass filter in front of the exit slit (black trace in Fig. 1a); the sub-bandgap peak, which would not be affected by this filter if it were genuine, is removed together with the supra-bandgap signal.

Importantly, when a different grating was used in the otherwise identical setup, the fractional harmonics did not appear, and the sub-bandgap peak present in Fig. 1a also is not observed in Fig. 1c. This shows that the appearance of the sub-bandgap peak in Fig. 1a is due to a defective grating.

The above discussion is not limited to SPS but applies to any spectroscopy using a grating monochromator. However, SPS is particularly sensitive to leaked photons (regardless of their origin) since the measured signal is voltage, which increases logarithmically with light intensity compared with a current signal which normally varies linearly with intensity. This means that a very low intensity light input will give a relatively large voltage signal compared to the same intensity light used for a current measurement (e.g. photocurrent spectroscopy).

Although the need to stabilize an SPV signal (usually in the dark but sometimes also under illumination) before running a spectrum is well-known, it is worth mentioning it briefly here as another source of error in acquiring SPV spectra. SPV spectra should be taken only after the starting signal has stabilized. It is common for drift of the signal to occur at the beginning of measurement and this drift can occur over a relatively long time span (tens of minutes or more is not uncommon).

Based on the above examples and discussion, we suggest protocols to detect and mitigate spurious signals in SPS measurements. Number 3 and the first part of number 4 are already standard operating protocols but we reemphasise them here for completeness.

1. Monitor the output spectrum (without using any filters) of the monochromator over several relevant set wavelengths for each grating in the monochromator as in Fig. 3. If a grating is in any way handled (e.g. in adjusting an existing grating or a new grating added), it is advisable to repeat this procedure and in any case, it should be repeated occasionally, e.g. once a year. This will pick up any leaked radiation not only from a faulty grating but from the complete monochromator system.

2. Since (real) sub-bandgap signals, even small ones, may contain useful information, consider increasing the measurement sensitivity in the sub-bandgap region if variable signal amplification is possible in the SPS system.

3. Use order-sorting longpass filters to remove second (and higher, if detected using #1) harmonics from the monochromator output.

4. Leave the sample in the dark measurement condition prior to the SPS measurement for sufficient time to stabilize the response and rule out time-dependent drift and/or actual changes in the surface properties. We also suggest measuring the work function of the probe with a standard like highly-oriented pyrolytic graphite (HOPG) before and after the measurement to monitor any changes in the measured work function (which could arise from changes in the sample and/or the probe).

Experimental Section

Details on the preparation of the FTO/TiO_2/$MAPbI_{3-x}Cl_x$ and SnO_2/$FA_{0.85}MA_{0.15}PbI_{0.85}Br_{0.15}$/spiro OmeTAD layers can be found in references 3 and 9, respectively. The SPS measurements in WIS were performed using a Kelvin-probe configuration with a Besocke Delta-Phi probe and controller. The sample was illuminated by a 600 W tungsten-halogen lamp with wavelength selection by a Spectra Physics 1/4 m monochromator. The SPS measurements in Oxford were performed using KP technology's Kelvin probe system where a supercontinuum white light source (NKT Super compact) is used as a light source and monochromator (Princeton instrument, SP-2150) to produce monochromatic light.

Acknowledgement: We thank T.Z. Markus for fruitful discussions, PN is supported by Marie Skłodowska-Curie actions individual fellowships (grant agreement number 653184). The authors thank Prof. David Cahen (WIS) for his invaluable comments on the manuscript and experiments. The Oxford SPS system

was funded by EPSRC. The authors thank Dr. N. Noel of Univ. Oxford for providing the SnO_2/$FA_{0.85}MA_{0.15}PbI_{0.85}Br_{0.15}$/spiro OmeTAD sample.

References:

(1) Kronik, L. Surface Photovoltage Phenomena: Theory, Experiment, and Applications. *Surf. Sci. Rep.* **1999**, *37* (1–5), 1–206.

(2) Kronik, L.; Shapira, Y. Surface Photovoltage Spectroscopy of Semiconductor Structures: At the Crossroads of Physics, Chemistry and Electrical Engineering. *Surf. Interface Anal.* **2001**, *31* (10), 954–965.

(3) Gatos, H. C.; Lagowski, J. Surface Photovoltage Spectroscopy—A New Approach to the Study of High-Gap Semiconductor Surfaces. *J. Vac. Sci. Technol.* **1973**, *10* (1), 130–135.

(4) Barnea-Nehoshtan, L.; Kirmayer, S.; Edri, E.; Hodes, G.; Cahen, D. Surface Photovoltage Spectroscopy Study of Organo-Lead Perovskite Solar Cells. *J. Phys. Chem. Lett.* **2014**, *5* (14), 2408–2413.

(5) Dittrich, T.; Awino, C.; Prajongtat, P.; Rech, B.; Lux-Steiner, M. C. Temperature Dependence of the Band Gap of $CH_3NH_3PbI_3$ Stabilized with PMMA: A Modulated Surface Photovoltage Study. *J. Phys. Chem. C* **2015**, *119* (42), 23968–23972.

(6) Dymshits, A.; Rotem, A.; Etgar, L.; Park, N.-G.; Herz, L.; Murakami, T.; Snaith, H. J.; Mori, S.; Hsu, C.-M.; Nazeeruddin, M. K.; et al. High Voltage in Hole Conductor Free Organo Metal Halide Perovskite Solar Cells. *J. Mater. Chem. A* **2014**, *2* (48), 20776–20781.

(7) Brenner, T. M.; Egger, D. A.; Kronik, L.; Hodes, G.; Cahen, D.; Weller, M. T.; Weber, O. J.; Henry, P. F.; Pumpo, A. M. Di; Hansen, T. C.; et al. Hybrid Organic—inorganic Perovskites: Low-Cost Semiconductors with Intriguing Charge-Transport Properties. *Nat. Rev. Mater.* **2016**, *1* (1), 15007.

(8) Mitzi, D. B.; Feild, C. A.; Schlesinger, Z.; Laibowitz, R. B. Transport, Optical, and Magnetic Properties of the Conducting Halide Perovskite CH3NH3SnI3. *J. Solid State Chem.* **1995**, *114* (1), 159–163.

(9) Correa Baena, J. P.; Steier, L.; Tress, W.; Saliba, M.; Neutzner, S.; Matsui, T.; Giordano, F.; Jacobsson, J.; Srimath Kandada, A. R.; Zakeeruddin, S. M.; et al. Highly Efficient Planar Perovskite Solar Cells through Band Alignment Engineering. *Energy Environ. Sci.* **2015**.

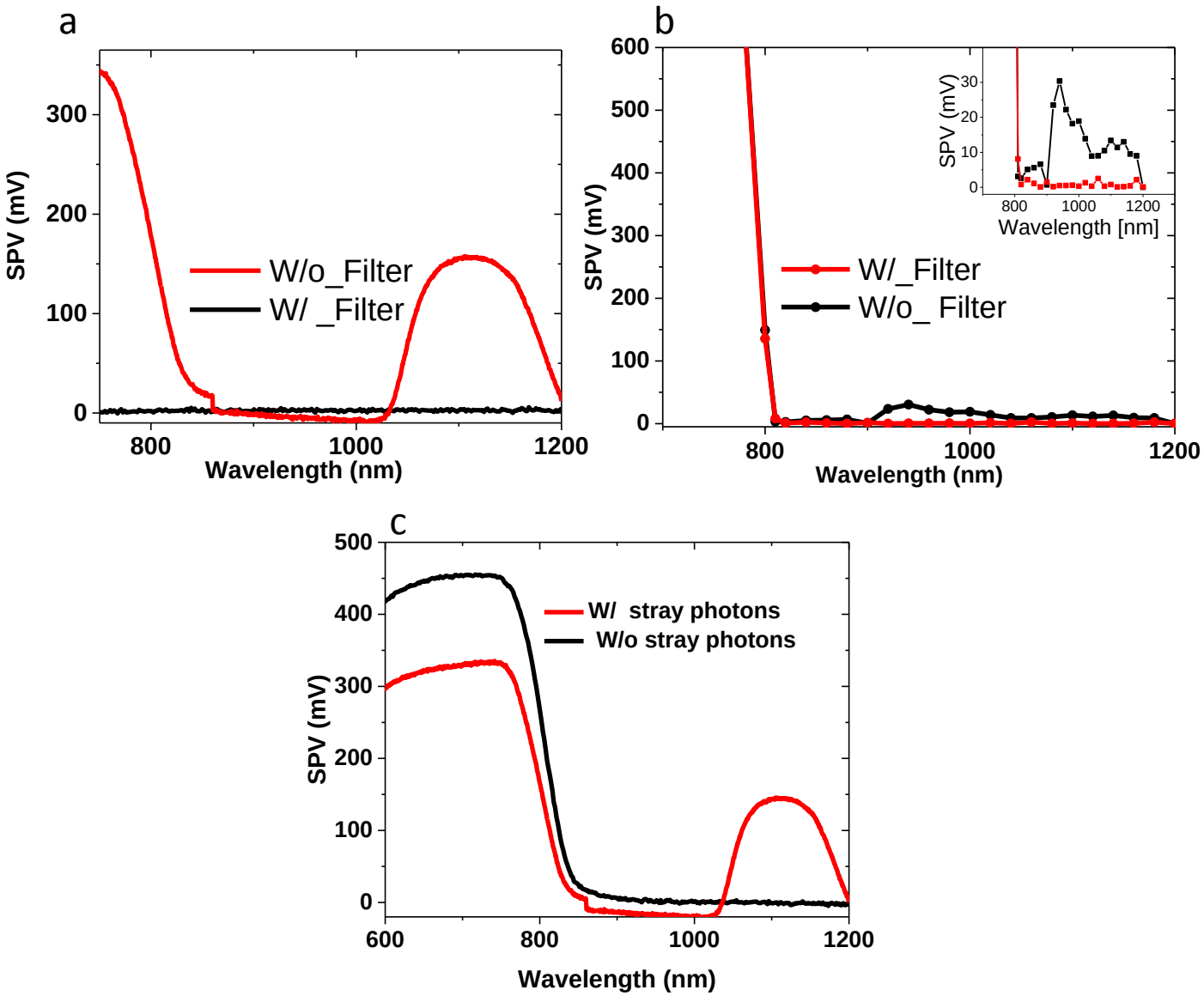

Figure 1 : (a) SPV spectrum of FTO/TiO_2/$MAPbI_{3-x}Cl_x$ (red line) recorded with the same set-up and under similar conditions as reported in reference 4 (including a 690nm longpass filter), SPV spectra of the same junction is shown with a 1025 nm longpass filter (black line) at the exit slit (Illumination from the perovskite side). (b) SPV spectrum without (black) and with (red) a 665 longpass nm filter of SnO_2/$FA_{0.85}MA_{0.15}PbI_{0.85}Br_{0.15}$/spiro OmeTAD junction. Illumination from the spiro OmeTAD side. (c) SPV spectrum of FTO/TiO_2/$MAPbI_{3-x}Cl_x$ recorded with a monchromator that leaks stray photons (red line) and after changing the optical apparatus (different grating) to reduce the amount of stray photons (black line). Both in (a) and (c) a 690 nm longpass filter was used in the region of 860-1200 nm.

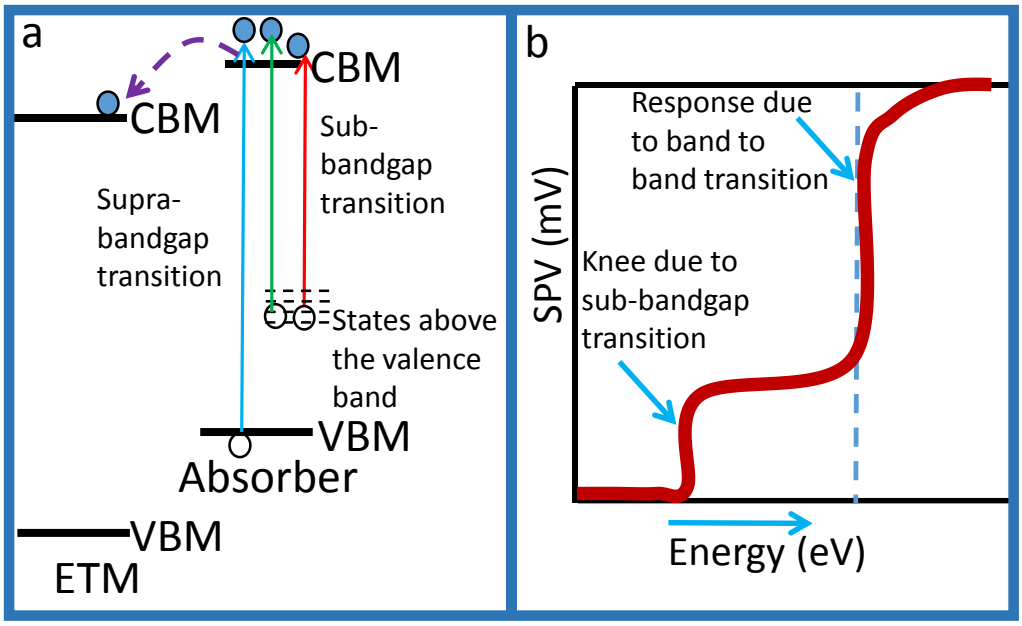

Figure 2 : (a) Schematic diagram showing a typical interface and transitions responsible for the SPV response. VBM = Valence band minimum, CBM = conduction band maximum, ETM = Electron transporting material, filled circles = electrons, empty circles = holes. For simplicity, we have shown the effect from the bulk and the interface. There may be some contribution from the surface which could be additive or subtractive to the SPV signal from the interface (see the supporting information in reference 4 for more information. (b) Corresponding schematic SPV spectrum of the interface described in (a).

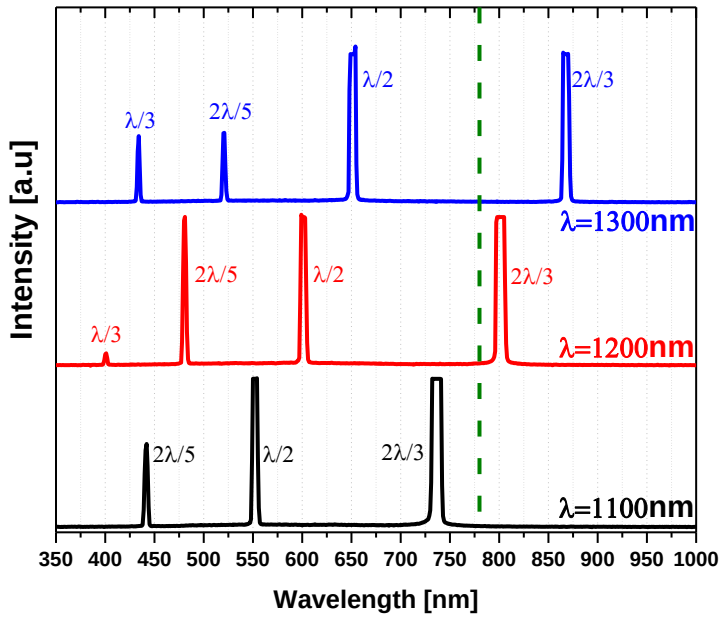

Figure 3: Measurement of the emitted light in the exit window of a double monochromator system. The set wavelengths are shown in the bottom right, the dashed green line represents $\lambda_{bandgap}$ of the MAPI (~780 nm).